

Detection of a novel gene mutation, ERBB2 exon 20 insertion, in bronchial adenoma using next-generation sequencing and a review of the literature

Qian Wu

Sichuan University West China Hospital

Lin Li

Sichuan University West China Hospital

Ke Zheng

Sichuan University West China Hospital

Yuan Tang

Sichuan University West China Hospital

Lili Jiang (✉ 879876047@qq.com)

Sichuan University West China Hospital

Research

Keywords: Ciliated muconodular papillary tumor, Bronchial Adenoma, next generation sequencing, ERBB2

Posted Date: June 16th, 2020

DOI: <https://doi.org/10.21203/rs.3.rs-21235/v2>

License:  This work is licensed under a Creative Commons Attribution 4.0 International License. [Read Full License](#)

Abstract

Objectives: Ciliated muconodular papillary tumor (CMPT) is a rare peripheral lung tumor and is a subtype of bronchial adenoma (BA). Although recent studies have suggested that BA is a neoplastic disease, the complete histogenesis of BA is not fully understood and molecular data are limited.

Methods: We examined the clinicopathological features of four patients with BA and performed immunohistochemical analysis and next-generation sequencing to characterize the molecular features of BA. A review of the previous literature was also undertaken to comprehensively conclude the molecular characteristics of this disease.

Results: From previous studies and the present study, 99 BA /CMPT cases have been reported to date, with most of the patients from East Asia (77/99, 77.8%). The median age was 64 years old and the ages ranged from 19 to 84 years. The proportion of males and females was close, being approximately 1:1.3. From the computed tomography images, the BA /CMPT tumor usually presented as a peripheral solid mass, part-solid nodules, or ground-glass opaque with an irregular border and occasional central cavities. ERBB2, EGFR, BRAF, and AKT1 mutations were found on the computed tomography images of the BAs. To the best of our knowledge, this is the first study to report about ERBB2 exon 20 insertion in BA.

Conclusion: BA /CMPT is a rare pulmonary disease that mainly affects elderly Asian patients. Many abnormal molecular changes were found, which confirmed the neoplastic nature of BA /CMPT. However, it also added to the debate regarding the biological behavior of BA /CMPT.

Introduction

Ciliated muconodular papillary tumor (CMPT) is a newly recognized peripheral lung disorder, which was first described in 2002 by Ishikawa et al. [1]. CMPT was once considered a very rare tumor, mainly affecting East Asian patients. However, in recent years, many cases have been reported with increasing recognition of this tumor [2-26]. Kamata reported 10 cases in 2015 [6] and both Chang (Western country cohort) [18] and Zheng [19] reported more than 20 cases in 2018. To date, nearly 100 cases have been reported in the literature and most of these patients reside in East Asia countries. Thus, this tumor may not be as rare as once believed.

CMPTs often affect middle-aged to elderly adults and consist of ciliated columnar, mucous, and basal cells. The tumor is commonly surrounded by extracellular mucin pools in the peripheral lung. Some cases did not fit all diagnostic criteria, such as the absence of papillary architecture or the lack of mucinous and/or ciliated cells; however, they shared the histological features of having a bilayered bronchiolar-type proliferation and continuous layer of basal cells, which have been termed “non-classic” CMPTs by Zheng et al. [19]. Both Zheng et al. [19] and Chang et al. [18] found that these lesions also shared genomic abnormalities. Chang et al. [18] proposed a new group of tumors called bronchial adenoma (BA) in 2018 and sub-categorized BA into two groups: proximal-type and distal-type based on morphological and immunohistochemistry (IHC) factors. Hence, classic CMPTs only represent a subset of proximal-type BA. So we refer to the tumor as BA in this study.

To date, accumulating evidence has shown that BA/CMPT is a neoplastic disease; however, its histogenesis and biological behavior remain unknown and its molecular data are limited. Recent studies have identified *BRAF*, *ALK*, *EGFR*, *KRAS*, *HRAS*, and *AKT1* mutations in BA [7, 8, 13-16, 18, 19, 25, 26]. Among them, the most common driver mutations are *BRAF*^{V600E} mutations.

Here, we report four cases with BA. For all cases, molecular analysis using next-generation sequencing (NGS) was performed and *ERBB2*, *BRAF*, *AKT1*, and *EGFR* gene mutations were identified. To the best of our knowledge, this is the first study to report the existence of *ERBB2* mutation in BA /CMPT.

Materials And Methods

Clinical samples

The four cases were diagnosed at the West China Hospital of Sichuan University between 2017 and 2019. Clinical data were extracted from the electronic medical records of the hospital. The samples were fixed in 10% formalin, embedded in paraffin, and stained with hematoxylin and eosin. The clinical and pathological records were analyzed retrospectively and histological analysis was performed on the surgically resected specimens.

Immunohistochemical analysis

Immunohistochemical analysis was performed on the paraffin-embedded sections using the following primary antibodies: CK7 (clone RN7, BIO), CK20 (clone EP23, BIO), TTF-1 (clone 8G7G3/1, ZECA), p63 (clone UMAB4, BIO), and MIB-1 (clone MIB-1, DAKO). All staining procedures were performed on a Leica Bond-Max or Roche Ventana. PBS (Phosphate-Buffered Saline) was routinely used as a negative control.

Isolation of genomic DNA

The slides were reviewed by two experienced pathologists and the proportion of tumor tissues was evaluated. Paraffin-embedded tissue blocks corresponding to slides with a tumor proportion that was greater than 80% were chosen for DNA extraction and the genomic DNA was extracted using a QIAamp DNA FFPE kit (Qiagen; Germany). The concentration and quality were determined using a ScanDrop 200 spectrophotometer (Analytik Jena; Germany), with a minimum of 200 ng of DNA required for NGS library construction. The optical absorbance of wavelength 260 nm and wavelength ratio of wavelength 260–280 nm were calculated.

Capture-based targeted DNA sequencing

DNA splicing was performed using a Covaris M220 (Covaris; MA, USA), followed by terminal repair, phosphorylation, and adaptor ligation. Agencourt AMPure XP beads (Beckman Coulter; Brea, CA, USA) were used for purification, followed by enrichment with 56 target genes (including *AKT1*, *ALK1*, *ARAF*, *ATM*, *BIM*, *BRAF*, *BRCA1*, *BRCA2*, *CCND1*, *CDK4*, *CDK6*, *CDKN2A*, *CTNNB1*, *CYP2C19*, *CYP2D6*, *CYP3A4*, *DDR2*, *DPYD*, *EGFR*, *ERBB2*, *ERBB3*, *ERBB4*, *FGF19*, *FGF3*, *FGF4*, *FGFR1*, *FGFR2*, *FGFR3*, *FLT3*, *HRAS*, *JAK1*, *JAK2*, *KDR*, *KIT*, *KRAS*, *MAP2K1*, *MET*, *MTOR*, *NRAS*, *NRG1*, *NTRK1*, *NTRK2*, *NTRK3*, *PDGFRA*, *PIK3CA*, *PCTH1*, *PTEN*, *RAF1*, *RET*, *ROS1*, *SMO*, *STK11*, *TP53*, *TSC2*, *TSC1*, and *UGT1A1*). A Qubit 2.0 fluorimeter with a dsDNA high-sensitivity assay kit (Life Technologies; Carlsbad, CA) were used to assess the quality and size of the fragments. The data of quality control is shown in Supplementary table. Qualified samples were sequenced on a Miseq (Illumina, Inc.; USA) with paired end reads and an average sequencing depth of 300×.

Gene mutation analysis

The sequence data were analyzed as previously described [27]. Sequence data were mapped to the reference human genome (hg19) using a Burrows-Wheeler Aligner. Alignment and variant calling were performed using a Genome Analysis Tool Kit and VarScan. Variants were filtered using the VarScan ffilter pipeline, loci with a depth less than 100 were filtered out. Single nucleotide variants (SNVs) and short insertions/deletions (indels) were identified using VarScan2, with a minimum variant allele frequency threshold set at 0.01 and a p-value threshold for calling variants set at 0.05 to generate variant call format files. All SNVs/indels were annotated using ANNOVAR and each SNV/indel was manually checked on an Integrative Genomics Viewer.

Results

Clinical characteristics

Three of the four patients were female and one was male, with an age range from 32 to 65 years. The male patient had a history of smoking, whereas all female patients did not. All four patients were found to have pulmonary nodules by physical examination. Computed tomography (CT) imaging showed solid or ground-glass nodules in the peripheral lung. The volume of all tumors in the studied cases was less than 1 cm in diameter.

All cases received wedge resections either at the West China Hospital of Sichuan University or other hospitals. The detailed clinicopathological features are shown in Table 1. Some cases were misdiagnosed at first. Case 2 was originally diagnosed as atypical alveolar epithelial hyperplasia and suspected adenocarcinoma from the frozen section. Case 3 was misdiagnosed as mucinous adenocarcinoma. Two patients had combined diseases: case 1 had metastatic invasive ductal carcinoma of the breast and adenocarcinoma in situ (AIS) of the lung, whereas case 3 had a minimally invasive adenocarcinoma of the lung.

Pathological features

Gross examination of the tumors in the four cases showed a well-demarcated gray-white solid mass. Microscopically, our cohort consisted of two proximal-types and two distal-types of BA. The tumors were composed of various proportions of ciliated columnar, mucus, and continuous basal cells with surrounding mucous lakes (Fig. 1A). The nuclear atypia was mild and mitosis and necrosis were not found. Muscular arteries were often seen in the center of the tumor (Fig. 1A), indicating that the tumor was localized around the bronchioles.

One proximal-type case showed predominantly papillary architectural patterns (Fig. 1B) and the other showed predominantly adherence architectural patterns with an occasional papillary structure (Fig. 1A & C). The ciliated columnar cells were easily found in this subtype (Fig. 1C). The distal-type cases revealed adherence and glandular architecture, the papillary structure was not obvious, and there was a lack of ciliated columnar cells (Fig. 1D-F).

Both the proximal and distal growth patterns revealed a skipping growth pattern (Fig. 1A, D) at the edge of the tumor and the micropapillary tufts were detached into the alveolar cavities (Fig. 1C, F). In addition, we found fibrous tissue hyperplasia and lymphocytes and plasma cells infiltrating in the focal areas (Fig. 1E).

Immunohistochemistry

All tumor cells were positive for CK7 (Fig. 2A); however, they were negative for CK20 (Fig. 2B), whereas the basal cells were positive for P63 (Fig. 2C). Consistently, the Ki67 index was less than 5% (Fig. 2D), indicating a relatively indolent biological behavior. For the proximal-type BAs, a few ciliary and basal cells were weakly positive for TTF-1 (Fig. 2E), whereas the distal-type BAs were strongly positive for it (Fig. 2F).

Molecular analysis

All cases underwent NGS to profile the molecular abnormalities (Table 1). Case 1 harbored *ERBB2* exon 20 insertion in the BA. Case 2 contained detected *EGFR* mutations. Case 3 was negative and case 4 harbored *BRAF* and *AKT1* mutations. The detailed information of these detected mutations are shown in Table 2.

NGS was performed on the BA sample, as well as on the metastatic breast cancer and AIS of the lung tissues for case 1. Consequently, multiple gene mutations were detected in the breast cancer metastatic focus including *KRAS*-ex2-G12A (48.82%), *PIK3CA*-ex21-H1047R (45.53%), *TP53*-ex5-V173L (42.76%), and *ATM*-ex18-C907F (27.64%), and there was an increase in the *KRAS* copy number (copy number = 3.51). However, no *ERBB2* mutation was found; therefore, the *ERBB2* exon 20 insertion was unique for BA. Unfortunately, DNA could not be extracted from the AIS tissue because of the limited sample amount.

Discussion

BA is a newly described tumor defined by Chang et al. [18], which is a more extensive terminology than that of CMPT. It has not been well recognized by pathologists and cannot be classified according to the 2015 WHO classification system [28]. A total of 26 previous studies about this family of neoplasms were searched in the literature, plus the cases in the present study, from which 99 cases of BA /CMPT were reported. The clinicopathological features of these cases are summarized in Table 3.

BA often affects middle-aged to elderly adults from East Asia (77/99, 77.8%), with the median age being 64 years old (range from 19 to 84 years old). The incidence rate of male and female is similar, being close to 1:1.3. BA occurs almost exclusively in the peripheral lungs. Chest CT images showed peripheral solid mass, part-solid nodules, or ground-glass opacity with an irregular border, and some of the patients showed a central cavity [3, 6, 9, 10, 16, 17, 19, 21, 23, 24]. The median diameter was 0.9 cm (range 0.2 to 4.5 cm), mostly between 0.2 and 2 cm. Only two cases were 3.5 cm and 4.5 cm in diameter [11].

Typically, the tumor is a pale mucinous nodule with an irregular border and sometimes a central cavity is found in the resected specimens. Histologically, BA /CMPT displays diverse morphological patterns including adherence, glandular, papillary, and micropapillary architecture, with abundant mucin around the tumor and the mucinous pool spreading into the adjacent alveolar spaces. The tumor is mainly composed of mucous and basal cells, while ciliated columnar cells may be present or absent. A few cells showed apical cytoplasmic snouts similar to club (Clara) cells [18]. The tumor cells lacked nuclear atypia, mitosis, and necrosis. Chang et al. [18] reported 25 lesions from 21 patients, with most of the lesions being flat and only seven lesions containing focal papillary architecture. They categorized the lesions into two groups: proximal-type and distal-type based on the morphological and IHC similarities of the bronchiolar structures. The classical CMPT belongs to the proximal-type BA and the TTF1 staining is negative or weakly positive. However, for distal-type BAs, the TTF1 and Napsin A show diffuse positivity.

Some cases revealed discontinuous (skipping) growth patterns, which resembled the spread of tumors through air spaces and micropapillary tufts detached in the alveolar cavity, which is similar to micropapillary adenocarcinoma. Chang et al. [18] hypothesized that these cells were interconnected with each other in 3-dimensional spaces because these skip lesions do not extend away for more than a few alveoli and the basal cells were always present. However, these microscopic features of BA /CMPT may be an extreme diagnostic challenge for pathologists, especially when studying intraoperative frozen sections.

Immunohistochemically, the three types of cells strongly expressed CK7, and always expressed CEA, HNF4 α , MUC1, MUC5B, and MUC5AC [3, 5, 9, 11, 12, 15], which is consistent with primary lung adenocarcinoma. The ciliated columnar cells were focally positive for MUC5AC, whereas the mucous cells lacked staining for MUC5AC. Some of the cases showed positive membrane staining for β -catenin [9]. The tumor cells were always negative for CK20, CDX-2, P53, MUC2, and MUC6, and had a low ki-67 index, usually less than 10% (often less than 1%) [2, 3, 5, 9-12, 15, 17]. The basal cells were positive for p63 and CK5/6.

Previously reported gene mutations of BA CMPT are summarized in Table 4. Several molecular alterations have been identified in BAs, including *BRAF*, *EGFR*, *KRAS*, *ALK* rearrangement, *AKT1*, and *HRAS* (Table 4). Consistent with these, we performed molecular analysis on our four cases and found *EGFR*, *BRAF*, and *AKT1* mutations. To the best of our knowledge, this is the first study to report the existence of *ERBB2* mutation in BA CMPT. As shown in Figure 3, the most common mutation was *BRAF*^{V600E} (38%), followed by *EGFR* (15%), *KRAS* (12%), *ALK* rearrangement (4%), *AKT1* (4%), *HRAS* (1%), *BRAF*^{G606R} (1%), and *ERBB2* (1%).

Human epidermal growth factor receptor 2 (*HER2/ERBB2*) is a receptor tyrosine kinase of the *ERBB* family, which plays a significant role in cancer development and progression, especially in breast, ovarian, and gastric cancers. The overexpression of HER2 protein is associated with poor prognosis. Recent studies have shown that the *HER2* mutation is a distinct subset of lung adenocarcinomas. *ERBB2* mutations are exclusive to *EGFR/KRAS/ALK* mutations and represent 6% of *EGFR/KRAS/ALK* negative specimens of non-small cell lung cancers (NSCLC). In NSCLCs, the most common mutations of *ERBB2* are in-frame insertions in exon 20 and are more frequent among non-smokers [29]. There is some overlap on genetic changes between BA and NSCLC. However, for all patients, there was no recurrence or metastasis after 2–120 months of follow-up. However, this type of disease often leads to misdiagnosis because they may morphologically mimic mucinous adenocarcinoma.

Of the 99 patients, 23 were originally diagnosed with adenocarcinoma (23.0%) [6, 17-19, 5, 21, 23, 24] and two were suspected of having malignant tumors (2.0%) [6]. Furthermore, some cases were only pathologically descriptive diagnoses. Therefore, pathologists must distinguish BA /CMPT from malignant tumors, especially during intraoperative diagnosis. The well-differentiated mucinous adenocarcinoma can have ciliated columnar cells especially when adenocarcinoma infiltrates into the bronchioles; however, basal cells are never present. Evidence support of malignancy should be carefully ruled out and immunohistochemical analysis highlighting basal cells with p63 and/or CK5/6 is helpful. Otherwise, solitary peripheral ciliated glandular papilloma, mixed squamous cells, and glandular papilloma and mucoepidermoid carcinoma must be considered as differential diagnoses.

In conclusion, we reported four cases of BAs and detected the mutation of *ERBB2* exon 20 insertion for the first time. BA /CMPT is a rare peripheral tumor that exhibits characteristics similar to those of adenocarcinoma, including morphological and genetic changes. At present, BA shows benign biological features that might be due to the limited number of cases. The pathogenesis and biological behavior of BA /CMPT must be examined further in future research and requires the study of more cases and longer follow-up times.

Declarations

Availability of data and materials

The data used and/or analyzed during the present study are available from the corresponding author on reasonable request.

Acknowledgements

Not applicable.

Ethics approval and consent to participate

This study obtained the approval of the ethics committee of West China Hospital at Sichuan University. Written informed consent was obtained from each patient.

Consent for publication

Not applicable.

Competing interests

The authors declare that they have no competing interests.

Funding

This study was supported by the 1.3.5 Project for Disciplines of Excellence-Clinical Research Incubation Project, West China Hospital, Sichuan University (No. 2019HXFH002).

Authors' contributions

Q.W. and L.L. contributed equally to this work. Q.W. and L.L. wrote the manuscript, L.L. collected and reviewed all the cases; Q.W. performed data analysis and review; K. Z. performed the IHC; Y.T. performed the NGS; and L.J. revised the manuscript. All authors read and approved the final manuscript.

Abbreviations

AIS: Adenocarcinoma in situ

BA: Bronchial adenoma

CMPT: Ciliated muconodular papillary tumor

CT: Computed tomography

IHC: immunohistochemistry

NGS: next-generation sequencing

NSCLC: non-small cell lung cancers

References

1. Ishikawa Y. Ciliated muconodular papillary tumor of the peripheral lung: Benign or malignant? *Pathol Clin Med (Byouri-to-Rinsho)* 2002, 20: 964-5.
2. Harada T, Akiyama Y, Ogasawara H, Atsuo H, Kenzo O, Miyako H, Ishikawa Y: Ciliated muconodular papillary tumor of the peripheral lung: a newly defined rare tumor. *Respir Med* 2008, 1:3.
3. Sato S, Koike T, Homma K, Yokoyama A: Ciliated muconodular papillary tumour of the lung: a newly defined low-grade malignant tumour. *Interact Cardiovasc Thorac Surg* 2010, 11:685-7.
4. Hata Y, Yuasa R, Sato F, Otsuka H, Goto H, Isobe K, Mitsuda A, Wakayama M, Shibuya K, Takagi K: Ciliated Muconodular Papillary Tumor of the Lung: A Newly Defined Low-grade Malignant Tumor with CT Findings Reminiscent of Adenocarcinoma. *JPN J Clin Oncol* 2012, 2: 2.
5. Chuang HW, Liao JB, Chang HC, Wang, JS, Lin, SL, Hsieh, P: Ciliated muconodular papillary tumor of the lung: a newly defined peripheral pulmonary tumor with conspicuous mucin pool mimicking colloid adenocarcinoma: a case report and review of literature. *Pathol Int* 2014, 64: 352-7.
6. Kamata T, Yoshida A, Kosuge T, Watanabe SI, Tsuta, K: Ciliated Muconodular Papillary Tumors of the Lung: a clinicopathologic analysis of 10 Cases. *Am J Surg Pathol* 2015, 39: 753-60.
7. Kamata T, Sunami K, Yoshida A, Shiraishi K, Furuta K, Shimada Y, Katai H, Watanabe S, Asamura H, Kohno T, Tsuta K: Frequent BRAF or EGFR mutations in ciliated muconodular papillary tumors of the lung. *J Thorac Oncol* 2016, 11:261-5.
8. Liu L, Aesif SW, Kipp BR, Voss JS, Daniel S, Aubry MC, Boland JM: Ciliated muconodular papillary tumors of the lung can occur in Western patients and show mutations in BRAF and AKT1. *Am J Surg Pathol* 2016, 40:1631-6.
9. Kon T, Baba Y, Fukai I, Watanabe G, Uchiyama T, Murata T: Ciliated muconodular papillary tumor of the lung: A report of five cases. *Pathol Int* 2016, 66: 633-9.
10. Lau KW, Aubry MC, Tan GS, Chong, HL, Takano, AM: Ciliated muconodular papillary tumor: A solitary peripheral lung nodule in a teenage girl. *Hum Pathol* 2016, 49: 22-6.
11. Ishikawa M, Sumitomo S, Imamura N, Tomoki N, Katsutaka M, Kazuo O: Ciliated muconodular papillary tumor of the lung: report of five cases. *J Surg Case Reports* 2016, 8:8.
12. Chu HH, Park SY, Cha EJ: Ciliated muconodular papillary tumor of the lung: The risk of false-positive diagnosis in frozen section. *Hum Pathol Case Reports* 2017, 7:8-10.

13. Taguchi R, Higuchi K, Sudo M, Misawa K, Miyamoto T, Mishima O, Kitano M, Azuhata K, Ito N: A case of anaplastic lymphoma kinase (ALK)-positive ciliated muconodular papillary tumor (CMPT) of the lung. *Pathol Int* 2017, 67: 99–104.
14. Kim L, Kim YS, Lee JS, Choi SJ, Park IS, Han JY, Kim JM, Chu, YC: Ciliated muconodular papillary tumor of the lung harboring BRAF V600E mutation and p16INK4a overexpression without proliferative activity may represent an example of oncogene-induced senescence. *J Thorac Dis* 2017, 9: 1039-1044.
15. Udo E, Furusato B, Sakai K, Prentice LM, Tanaka T, Kitamura Y, Tsuchiya T, Yamasaki N, Nagayasu T, Nishio K: Ciliated muconodular papillary tumors of the lung with KRAS/BRAF/AKT1 mutation. *Diagn Pathol* 2017,12:1-5.
16. Jin Y, Shen X, Shen L, Sun Y, Chen H, Li Y: Ciliated muconodular papillary tumor of the lung harboring ALK gene rearrangement: Case report and review of the literature. *Pathol Int* 2017, 67:171–5.
17. Yan Wang, Shihong Shao, Yujun Li: Two cases of pulmonary ciliary mucinous nodular papillary tumors. *Chin J Pathol* 2017, 46: 268-270.
18. Chang JC, Montecalvo J, Borsu L, Lu SH, Rekhtman N: Expansion of the Concept of Ciliated Muconodular Papillary Tumors with Proposal for Revised Terminology Based on Morphologic, Immunophenotypic, and Genomic Analysis of 25 Cases. *Am J Surg Pathol* 2018, 42:1010-1026.
19. Zheng Q, Luo R, Jin Y, Shen XX, Shan L, Shen L, Hou YY, Li Y: So-called “non-classic” ciliated muconodular papillary tumors: a comprehensive comparison of the clinicopathological and molecular features with classic ciliated muconodular papillary tumors. *Hum Pathol* 2018, 82:193-201.
20. Isaila B , Ananthanarayanan V , Pambuccian SE: Ciliated Muconodular Papillary Tumor of the Lung: A New Entity Formerly Regarded as a Well-Differentiated Adenocarcinoma. *AJSP: Reviews & Reports* 2018, 23.
21. Uchida T, Matsubara H, Ohnuki Y, Sugimura A, Matsuoka H, Ichihara T, Nakajima H: Ciliated muconodular papillary tumor of the lung presenting with polymyalgia rheumatica-like symptoms: a case report. *AME Case Rep* 2019;3:1-4.
22. Yao X, Gong Y, Zhou J, Lyu M, Zhang H, Zhou H, Luo Q, Liu L: A surgical case of ciliated muconodular papillary tumor. *Thoracic Cancer* 2019,10:1019–1022.
23. Shen L, Lin J, Ren Z, Wang B, Zhao K, Lu Y, Wang F, Zhan L: Ciliated muconodular papillary tumor of the lung: report of two cases and review of the literature. *J Surg Case Rep* 2019,8: 1–3.
24. Cheung FMF, Guan J, Luo QG, Sihoe ADL, Shen XP: Ciliated muconodular papillary tumour of the lung mimicking mucinous adenocarcinoma: a case report and literature review. *Hong Kong Med J* 2019. 25:71–3.
25. Shao K, Wang YL, Xue Q, Mu J, Gao Y, Wang Y, Wang B, Zhou L, Gao S: Clinicopathological features and prognosis of ciliated muconodular papillary tumor. *J Cardiothorac Surg* 2019,14:1-7.
26. Kashima J, Hishima T, Tonooka A, Horiguchi SI, Motoi T, Okuma Y, Hosimi Y, Horio H: Genetic and immunohistochemical analyses of ciliated muconodular papillary tumors of the lung: A report of five cases. *SAGE Open Med Case Rep* 2019,7: 1-5.
27. Fu Y, Wu Q, Su F, Tang Y, Lin Y, Wang W, Jiang L; Novel gene mutations in well-differentiated fetal adenocarcinoma of the lung in the next generation sequencing era. *Lung cancer* 2018,124: 1–5.
28. Travis WDBE, Burke AP, Marx A, Nicholson AG: WHO Classification of Tumours of the Lung, Pleura, Thymus and Heart. Lyon: IARC Press, 2015.
29. Arcila ME, Chaft JE, Nafa K, Roy CS, Lau C, Zaidinski M, Paik PK, Zakowski MF, Kris MG, Ladanyi M: Prevalence, clinicopathologic associations, and molecular spectrum of ERBB2 (HER2) tyrosine kinase mutations in lung adenocarcinomas. *Clin Cancer Res* 2012, 18: 4910.

Tables

Table 1 Clinicopathologic features of the four BA patients

No.	Sex	Age	Site	Size(cm)	Smoking	Morphology subtype	Papillary structure	Mucinous cells	Cilia	Discontinuous distribution	Original diagnosis	Combined diseases	Mutation
1	F	49	RML	0.6	No	Proximal	predominant	Present	Present	Present	CMPT	IDC, AIS	<i>ERBB2</i> 20ins
2	F	65	RUL	0.6	No	Distal	A few	Present	absent	Absent	AC	None	<i>EGFR</i> ex19 del L747_S752
3	F	62	LUL	0.4	No	Distal	A few	Present	absent	Present	AC	MIA	None
4	M	32	LUL	0.8	Yes	Proximal	predominant	Present	Present	Present	NA	None	<i>AKT1</i> p.E17K, <i>BRAF</i> ^{V600E}

NA: not available. CMPT : Ciliated muconodular papillary tumor. IDC: invasive ductal carcinoma of breast. AIS: adenocarcinoma *in situ*. MIA: microinvasive adenocarcinoma. RML: right middle lobe. RUL: right upper lobe. LUL:left upper lobe.

No.	Sex	Age	Mutation genes	Mutation type	Exon rank	Mutation sites	Description	Allele frequency(%)
1	F	49	<i>ERBB2</i>	disruptive_inframe_insertion	20	c.2313_2324dup(p.Ala775_Gly776insTyrValMetAla)	p.A775_G776insYVMA	2.79
2	F	65	<i>EGFR</i>	conservative_inframe_deletion	19	c.2239_2256delinsCAA(p.Leu747_Ser752delinsGln)	p.L747_S752delinsQ	4.56
3	F	62	None	None	None	None	None	None
4	M	32	<i>AKT1</i>	missense_variant	4	c.49G>A(p.Glu17Lys)	p.E17K	5.39
			<i>BRAF</i>	missense_variant	15	c.1799T>A(p.Val600Glu)	p.V600E	6.40

Table 2 Molecular features of the four BA patients

Author[year]	No. of cases	Median age(y)	Race	Gender		Size (cm)	No. of smokers	Central cavity
				F	M			
Ishikawa et al. ^[11] (2002)	1	50	Asian	1	0	1.5	0	NA
Harada et al. ^[2] (2008)	1	62	Asian	0	1	0.9	1	0
Sato et al. ^[3] (2010)	2	59;67	Asian	1	1	0.7;0.6	1	1
Hata et al. ^[4] (2013)	1	76	Asian	1	0	0.7	0	0
Chuang et al. ^[5] (2014)	1	68	Asian	0	1	0.7	1	0
Kamata et al. ^[6] (2015)	10	62(56-78)	Asian	3	7	1.0(0.6-1.5)	5	3
Liu et al. ^[8] (2016)	4	76(60-83)	Asian (2) Caucasian (2)	3	1	0.7(0.4-1.2)	1	0
T. Kon et al. ^[9] (2016)	5	70(66-80)	Asian	2	3	0.9(0.7-1.3)	NA	3
Kah et al. ^[10] (2016)	1	19	Asian	1	0	1.2	0	1
Ishikawa et al. ^[11] (2016)	5	70(66-82)	Asian	2	3	1.3(0.5-4.5)	3	0
Chu et al. ^[12] (2017)	1	56	Asian	0	1	0.8	NA	0
Taguchi et al. ^[13] (2017)	1	84	Asian	1	0	1.0	0	0
Kim et al. ^[14] (2017)	1	72	Asian	0	1	0.9	1	0
Udo et al. ^[15] (2017)	4	67	Asian	4	0	1.1(0.8-2.5)	0	NA
Jin et al. ^[16] (2017)	1	59	Asian	1	0	0.8	0	1
Yan et al. ^[17] (2017)	2	53(50-56)	Asian	1	1	0.9(0.4-1.3)	NA	1
Chang et al. ^[18] (2018)	21	72 (55-83)	Asian (2) Caucasian (12) NA (7)	10	11	0.5(0.2-2.0)	16	NA
Zheng et al. ^[19] (2018)	21	55 (31-78)	Asian	15	6	0.7(0.4-2.0)	NA	8
Isaila et al. ^[20] (2018)	1	61	Caucasian	1	0	0.3	1	NA
Uchida et al. ^[21] (2019)	1	78	Asian	0	1	1.9	NA	1
Yao et al. ^[22] (2019)	1	67	Asian	1	0	1.2	NA	NA
Shen et al. ^[23] (2019)	1	58	Asian	0	1	1.1	NA	1
Cheung et al. ^[24] (2019)	1	61	Asian	0	1	1.0	1	1
Shao et al. ^[25] (2019)	2	58,66	Asian	2	0	0.7(0.6-0.8)	NA	0
Kashima et al. ^[26] (2019)	5	71(56-73)	Asian	3	2	0.9(0.8-1.8)	NA	NA
Present cohort	4	55.5(32-65)	Asian	3	1	0.6(0.4-0.8)	1	0
Total	99	64(19-84)	Asian (77) Caucasian (15) NA (7)	56	43	0.9(0.2-4.5)	32	21

Table 3. Clinicopathological features of 99 CMPT/BAs reported in previous literatures and our present cohort
NA: not available

Author[year]	No. of cases	Mutations
Kamata et al. ^[7] (2015)	10	<i>BRAF</i> ^{V600E} (4); <i>BRAF</i> ^{G606R} (1);deletions in exon 19 of <i>EGFR</i> (3)
Liu et al. ^[8] (2016)	4	<i>BRAF</i> ^{V600E} and <i>AKT1</i> (1)
Taguchi et al. ^[13] (2017)	1	<i>ALK</i>
Kim et al. ^[14] (2017)	1	<i>BRAF</i> ^{V600E}
Udo et al. ^[15] (2017)	4	<i>BRAF</i> ^{V600E} (1); <i>KRAS</i> (1); <i>AKT1</i> (1)
Jin et al. ^[16] (2017)	1	<i>ALK</i>
Chang et al. ^[18] (2018)	21	<i>BRAF</i> (8); <i>EGFR</i> (4); <i>KRAS</i> (5); <i>HRAS</i> (1)
Zheng et al. ^[19] (2018)	21	<i>BRAF</i> (8), <i>EGFR</i> (3), <i>KRAS</i> (1) <i>ALK</i> (1)
Shao et al. ^[25] (2019)	2	<i>KRAS</i> (1), <i>BRAF</i> ^{V600E} (1)
Kashima et al. ^[26] (2019)	5	<i>BRAF</i> ^{V600E} (3)
Present cohort	4	<i>ERBB2</i> (1); <i>EGFR</i> (1); <i>AKT1</i> and <i>BRAF</i> ^{V600E} (1)
Total	74	<i>BRAF</i> ^{V600E} (28); <i>EGFR</i> (11); <i>KRAS</i> (9); <i>AKT1</i> (3); <i>ALK</i> (3); <i>BRAF</i> ^{G606R} (1); <i>HRAS</i> (1); <i>ERBB2</i> (1)

Table 4. Summary of reported gene mutations in the previous literatures and our present cohort

Figures

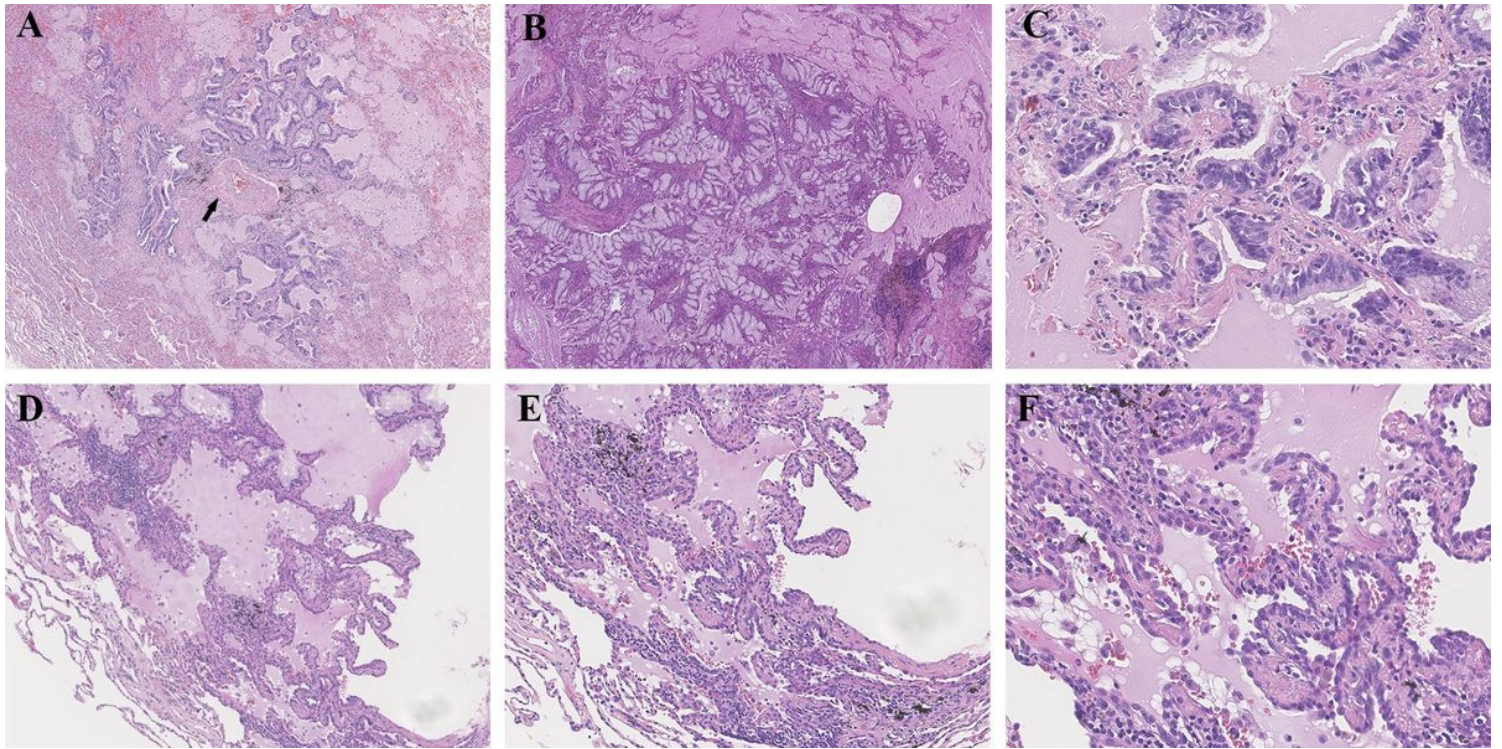


Figure 1

Morphology of BAs (A) Proximal-type BA: at low power, the tumor shows predominantly adherence architectural patterns with occasionally papillary structure and skipping growth pattern. Besides, massive mucous lake around and muscular artery in the center (arrow) are also presented ($\times 4$), (B) proximal-type BA with prominent papillary architectural pattern and massive mucous lake ($\times 20$), (C) proximal-type BA: at high power, the tumor is mostly consisted of ciliated and mucinous cells surrounded by basal cells, with lymphocytes in the stroma ($\times 40$), (D) distal-type BA: At low power, the tumor shows predominantly flat architectural patterns and massive mucous lake ($\times 4$), (E) distal-type BA: fibrous tissue hyperplasia, lymphocytes and plasma cells are showed in focal areas of stroma ($\times 20$), (F) distal-type BA: at high power, the tumor shows cuboidal cells that resemble type II pneumocytes, ciliated and mucinous cells are barely seen ($\times 40$).

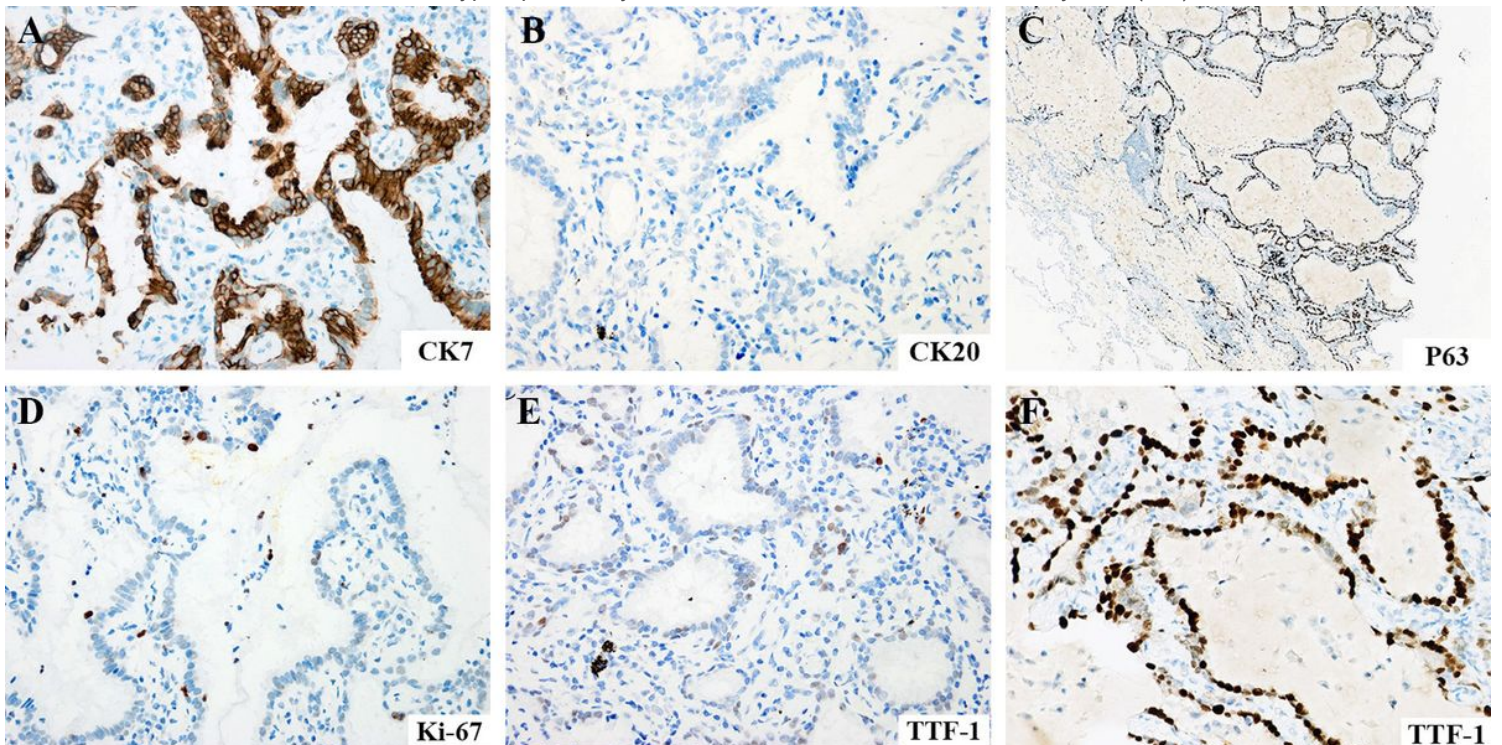


Figure 2

IHC of BAs (A) CK7 is strongly and diffusely positive in ciliated columnar cells and mucus cells (×40) (B) The tumor cells are negative for CK20 (×40), (C) At low power, P63 outlines the basal cells (×4) (D) The Ki-67 index of this tumor is low in this tumor, less than which is less than 5% (×40), (E) In proximal-type BA, ciliated columnar cells, mucus cells and basal cells shows weak and focal TTF-1 positivity (×40), (F) In distal-type BA, TTF-1 is strongly and diffusely positive (×40).

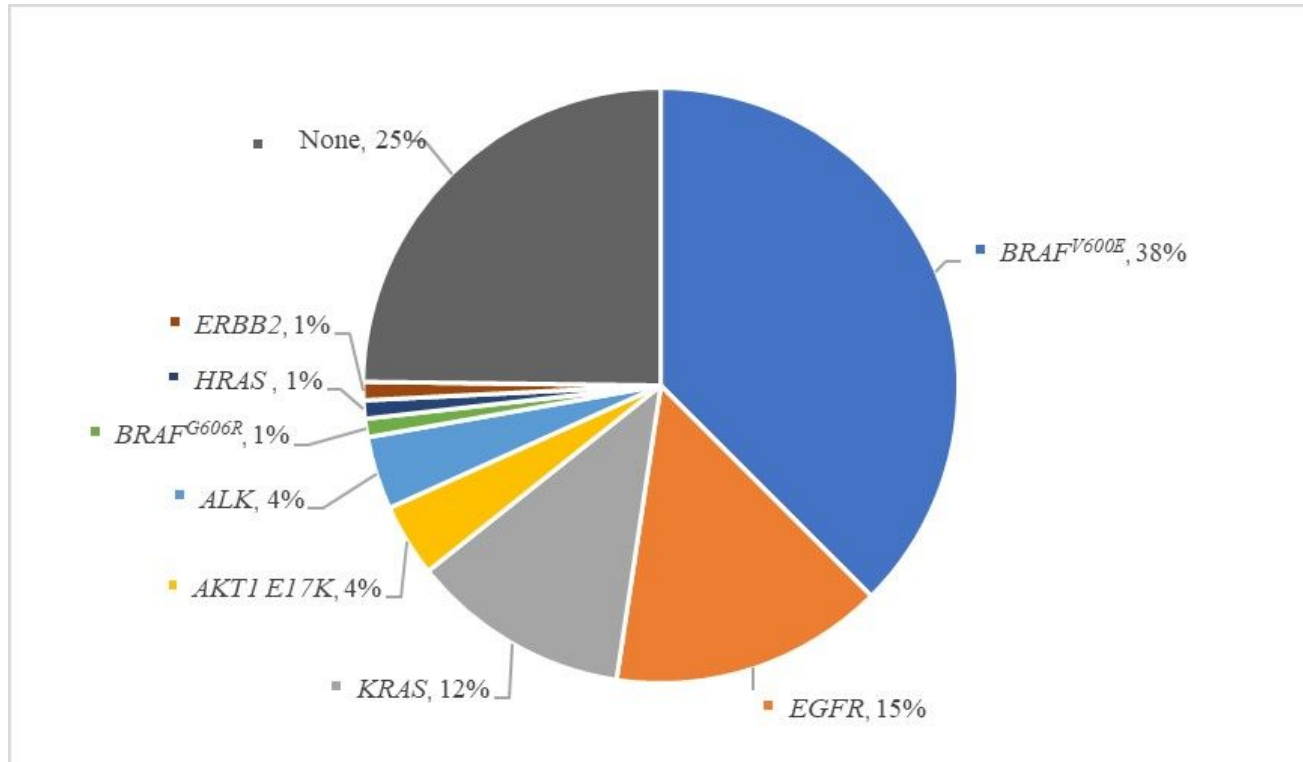


Figure 3

Molecular findings of BAs from previous studies and our present cohort.

Supplementary Files

This is a list of supplementary files associated with this preprint. Click to download.

- [Supplementarytable.docx](#)